IEEE Access
Multidisciplinary | Rapid Review | Open Access Journal

Received 17 May 2022, accepted 22 June 2022, date of publication 27 June 2022, date of current version 1 July 2022.

Digital Object Identifier 10.1109/ACCESS.2022.3186678

RESEARCH ARTICLE

Portable All-in-One Electroanalytical Device for Point of Care

HYUSIM PARK[1], YOUNGHUN PARK[1], SHANTHALA LAKSHMINARAYANA[1], (Graduate Student Member, IEEE), HYUN-MIN JUNG[2], MIN-YEONG KIM[2], KYU HWAN LEE[3], AND SUNGYONG JUNG[1], (Senior Member, IEEE)

[1]Electrical Engineering Department, The University of Texas at Arlington, Arlington, TX 76019, USA
[2]Electrochemistry Department, Korea Institute of Materials Science (KIMS), Changwon, Gyeongnam 51508, Republic of Korea
[3]Surface Technology Division, Department of Electrochemistry, Korea Institute of Materials Science (KIMS), Changwon 51508, Republic of Korea

Corresponding author: Sungyong Jung (jung@uta.edu)

ABSTRACT Recent technological advancements such as an expansion of available biomarkers and an incremental burden of chronic and infectious diseases made point of care (POC) devices in strong demand. It has a potential to surpass conventional lab-based devices in terms of time, cost, accessibility, and even accuracy. This potential strongly depends on an availability of affordable and miniaturized electronic POC devices that can provide a fast and sensitive response. This paper presents an all-in-one electroanalytical device (AED) which is a cost-effective, field-ready, and miniaturized electronic POC device integrated with the most commonly used electroanalytical techniques such as amperometric, voltammetric, potentiometric, conductometric, and impedimetric techniques. The proposed AED can analyze multiple electrochemical sensors simultaneously while having a very small size of 48 mm × 37 mm, including eight disposable screen-printed electrochemical sensor (SPES) connectors. The device supports wired communication using a universal serial bus (USB) and wireless communication with Bluetooth Low Energy (BLE). Furthermore, user-friendly customized Graphical User Interface (GUI) has been developed to control the device and send obtained data to the user. The system is evaluated through electrical tests to confirm the device accuracy. Subsequently, electrochemical experiments were conducted to evaluate device's performance in the field. These experiments indicated that the developed device operates as an electrochemical sensing device for POC applications. The proposed portable electroanalytical device can perform the most of electroanalytical methods in a single device which has very small form factor and capability to interpret multiple sensors at a time with user friendly interface.

INDEX TERMS Electroanalytical device, electrochemical readout, screen-printed sensor, point of care.

I. INTRODUCTION

The point of care (POC) system consists of a sensor to detect a target analyte and device to analyze the sensor data with user friendly interface capability as shown in Fig. 1, which have revolutionized many fields such as at-home patient care, disease management, and even the field to test the safety of water or food, since it can offer rapid diagnostic results in non-laboratory settings [1]–[3]. The quick provision of results can facilitate appropriate treatment or action promptly and save time and cost [4]. Not only will the POC devices produce an economic outcome but owing to the portability of devices, it also has a potential to allow wide distribution of service with relatively good quality across less developed regions [5]. Consequently, a global POC market size is projected to reach USD 50.6 billion by 2025 from USD 29.5 billion in 2020 [6]. This trend made a bold transition from bulky, protractive, and expensive sensors to cost-effective, miniaturized, portable, and highly sensitive sensors with short analysis time for various electrochemical sensors due to their

The associate editor coordinating the review of this manuscript and approving it for publication was Lei Wang.

FIGURE 1. Overview of electrochemical sensing application as the POC device.

easy operation [7], [8]. Electrochemical sensors are analytical devices that convert electrochemical reactions into applicable qualitative or quantitative signals such as current, voltage, or impedance. It has been applied and researched to detect trace amounts of a target, including small or large molecules, metal ions, bio-markers, etc. [9]–[12]. More specifically, a screen-printed electrochemical sensor (SPES) has acquired predominant importance as a miniaturized electrochemical sensor for the POC devices in the last decade, which is robust, cheap, tailorable, and mass-producible [13]–[17]. It is well-known that multi-analytes approach can provide more information for each single sample and it leads to faster and lower cost assays. For this approach, SPES can provide a powerful platform that has the ability to be functionalized and customized for the detection of different analytes [18]–[22]. Yáñez-Sedeño *et al*. published a comprehensive review on integrated affinity bio-sensing platforms which pays special attention to the importance of coupling multiplexed SPESs by utilizing various electrochemical measurement methods such as amperometry, Electrochemical Impedance Spectroscopy (EIS), and Square Wave Voltammetry (SWV) for simultaneous determination of biomarkers [20]. Malha *et al*. applied carbon black-modified SPES to detect nitrite and nitrate for environmental monitoring [21]. Having used Cyclic Voltammetry (CV), amperometry, and EIS analyses, they reported limit of detection values of 0.135 μM and with a linear range of detection of 0.3 μM – 18.8 μM. Attoye *et al*. demonstrated a simple, low-cost deoxyribonucleic acid (DNA) biosensor employed on SPES array to perform parallel measurement of DNA hybridization to quantify mutant genetic sequences. Both CV and EIS analyses were performed to determine whether consistent behavior was observed [22].

On the strength of growing interest of POC devices, numerous electroanalytical devices that can accommodate the electrochemical sensors and have capability to conduct multiple electroanalytical methods, have been studied and presented in the literature along with the sensor development [23]–[32]. Generally, the particular criteria known by the acronym ASSURED – (Affordable, Sensitive, Specific, User-friendly, Rapid and Robust, Equipment-free, and Deliverable to end-users) released by World Health Organization (WHO) in 2003 should be met to be considered as POC devices [33]. To satisfy the ASSURED criteria, most papers constructed their device with commercial off-the-shelf components, which is the most affordable way to build miniaturized devices at the minimum cost for various applications. Among those developed devices, a few papers introduced devices that can perform multiple electroanalytical methods to provide higher accuracy or utilize the devices to analyze multiple types of electrochemical sensors or biosensors. For instance, Ainla *et al*. developed Universal Wireless Electrochemical Detector by utilizing a Microcontroller Unit (MCU) which has an integrated Bluetooth Low Energy (BLE) [25]. The developed device can conduct multiple electroanalytical techniques like potentiometry, Chronoamperometry (CA), CV, and SWV. In a different approach, Glasscott *et al*. described a device, called SweepStat, capable of transacting CV, Linear Sweep Voltammetry (LSV), CA, chronocoulometry for two-electrodes sensor. It is able to interface with laboratory virtual instrument engineering workbench (LabVIEW^{TM}), one of the most popular software for applications requiring measurement in chemistry labs. Another researcher group, Jenkins *et al*. proposed battery-operated ABE-Stat embodied with CV, Differential Pulse Voltammetry (DPV), and potentiometric techniques while having Wireless Fidelity communication [30].

Most of the previously developed electrochemical readout devices require a few more external active components other than MCU to establish the analytical methods, making them large, expensive, and consuming high-power. Moreover, they are only able to measure one sensor at a time. However, the multiplexing capability becomes an important metric for the recent POC devices because, in many scenarios, measuring multiple biomarkers or analytes can improve diagnostic accuracy [3], [34], [35]. In this work, an All-in-one Electroanalytical Device (AED) that can perform CV, LSV, Anode Stripping Voltammetry (ASV), SWV, amperometry, CA, conductometry, potentiometry, and EIS for eight SPESs at a time is proposed. It is one of the devices that have the most diverse electroanalytical methods, while it requires only one component, MCU, to establish proposed methods, which makes the device to have a very small form factor and low-power consumption. Not only can the AED conduct multiple electroanalytical methods, but it can also analyze eight sensors simultaneously for high accuracy which is a one of the strong points of this work. The AED includes wired and wireless communication capability as a user-friendly device. Furthermore, a customized Graphical User Interface (GUI) to control the device and send the data to a personal computer (PC) has been developed.

II. SYSTEM DESIGN

A. ELECTROCHEMISTRY

The proposed device can perform the most common electroanalytical methods used in analytical chemistry and industrial processes: voltammetry, amperometry, conductometry, potentiometry, and impedimetry. In voltammetry, information about an analyte is obtained by measuring the current as the

potential is varied. The analytical data for the voltammetric experiment comes in the recognizable form of a voltammogram which plots the measured current produced by the analyte reaction against the provided potential. As voltammetry experiment, CV, SWV, LSV, and ASV are embedded in the proposed device, which can be re-categorized by provided potential type. Meanwhile, the amperometry measures the current generated from the activity of redox species at the interface wherein a fixed voltage is applied. As an amperometry type of analytical method, amperometry and CA are embarked in the proposed device. The conductometry is a method in which either there are negligible or no electrochemical reactions on the electrodes. It measures conductance that can be calculated utilizing current ratio that flows to the potential difference present which is the reciprocal of the resistance. Potentiometry is a technique usually used to find the concentration of a solute in a solution. In this technique, the potential between two electrodes can be measured using a high-impedance voltmeter to ensure that current flow at the electrodes is negligible so that the system is in equilibrium. Lastly, the EIS analyzes both faradaic and capacitive contributions in the electrochemical reaction at the electrode/solution interface and it measures the AC signal when sinusoidal perturbance is applied, often a potential at different frequencies. The impedance represents the opposition to an alternating current flow in an electrochemical cell. It is defined as the total resistive charge of the system, given by the sum of reactance and resistance.

B. PROPOSED SYSTEM DESIGN

Fig. 2 illustrates the block diagram of the proposed AED. The AED consists of SPES connector, analog multiplexer (AMUX), MCU, USB, and BLE module. The design of AED is largely inspired by Lopin's PSoC-Stat [31], which utilizes a versatile Programmable System on a Chip MCU 'CY8C5888LTI-LP097' (Cypress Semiconductor, CA, USA). The MCU includes necessary analog components such as analog to digital converter (ADC), digital to analog converter (DAC), operational amplifier (OP-AMP), and transimpedance amplifier (TIA), which are essential blocks to build electrochemical analytical methods. For small form factor, low power consumption, and low cost, the proposed design selected the 'CY8C5888LTI-LP097' as the MCU. Meanwhile, to accommodate multiple sensors in a single device, external precision complementary metal-oxide-semiconductor type AMUXs 'TMUX1208' (Texas instrument, TX, USA) are embodied to each working electrode (WE), reference electrode (RE), and counter electrode (CE) followed by the MCU. The chosen AMUX has very low on and off leakage currents and low charge injection, allowing high-precision measurement. It only consumes 10 nA, which is suitable for low-power applications and its on-resistance is 5Ω. Wired and wireless communication are supported to make the device user-friendly. To support wireless communication, the BLE module 'SPBTLE-1S' (STMicroelectronics, Geneva, CH) with an integrated onboard chip antenna is

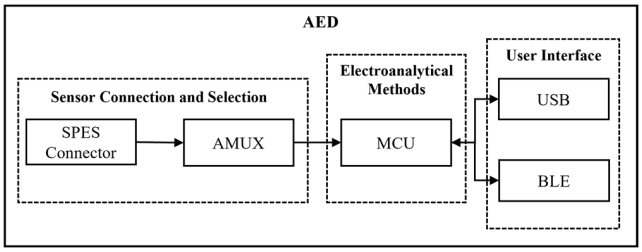

FIGURE 2. Block diagram of the proposed device.

employed for a small form factor. When the BLE module consumes 15 mA in maximum transmission mode with + 4 dBm transmit power while it only consumes 500 nA in standby mode. Either rechargeable 3.7 V lithium-ion polymer battery or universal serial bus (USB) can be utilized to power up the device. The proposed AED can perform the experiments where the sensor's outputs are within a voltage range of ± 2 V or a current range of ± 100 μA. It can collect data from eight of 3 or 2 electrodes SPESs simultaneously. The specification comparison of the proposed device with other existing devices is presented in Table 1. It clearly indicates that the proposed AED can measure the most various electroanalytical methods in a single device with a small size of 48 mm × 37 mm including 8 number of SPES connectors. Without the connectors, the proposed design consumes an area of 27 mm × 37 mm. All the electroanalytical methods are realised with internal blocks of the MCU by firmware development for small form factor, cost-efficiency, and low power consumption. The firmware of the MCU is developed in PSoC Creator 4.1, published by Cypress Semiconductor. Step by step explanation about the firmware development for establishing electroanalytical methods in the proposed AED will be discussed in later subsections.

1) VOLTAMMETRY, CONDUCTOMETRY, AND AMPEROMETRY

The voltammetry, conductometry, and amperometry methods require circuits for potential control and current measuring since those methods measure a varied current sensor output (I_{sensor}) due to chemical reactions, wherein a certain potential is applied to the sensor. These circuits are realized by MCU's internal ADC, DAC, OP-AMP, and TIA in a firmware as shown in Fig. 3. As potential control circuit, DAC and OP-AMP are used to apply a certain potential to the sensor. The potentiostat, which is realized with OP-AMP, passes a current through the CE until a voltage on the RE becomes the same voltage as the DAC. The positive input of OP-AMP is connected to DAC, and the negative input of the OP-AMP is connected to RE through AMUX to provide the constant potential while OP-AMP output is connected to CE. Also, to perform the measurement at negative potential conditions with a single power supply, a virtual ground concept is adopted by implementing DAC. The DAC is fed into the negative input of the ADC and positive pin of a TIA to make a virtual ground at 2.048 V, which is the middle of

TABLE 1. Specification comparision of existing devices with the proposed device.

Ref	Electroanalytical methods	MCU	Voltage range	Current range	EIS frequency	Sensor channel	Size (mm^2)	Year
This work	CV, LSV, ASV, SWV, Amperometry, CA, Conductometry, Potentiometry, EIS	CY8C5888LTI-LP097	±2V	±100 μA	512Hz – 80kHz	8	48 × 37	2022
[23]	CV, SWV, DPV	ATxmega256A3U	±1.5V	±10 μA	N/A	1	92 × 84	2015
[24]	CV, ASV, CA	ATxmega32E5	±1.2V	±100 μA	N/A	1	27 × 20	2019
[25]	CV, CA, SWV	RFD22121	±1.5V	±180 μA	N/A	1	N/A	2018
[27]	CV, LSV, CA	Arduino Teensy 3.2	±1.5V	±1.5 μA	N/A	1	N/A	2020
[30]	CV, DPV, Potentiometry, EIS	ESP8266	±1.65V	N/A	0.1 Hz – 100kHz	1	N/A	2019
[31]	CV, ASV, Amperometry,	CY8C5888LTI-LP097	±2V	±100 μA	N/A	1	108.9 × 24.1	2018
[36]	CV, SWV, Amperometry	ATmega2560	±1V	±400 μA	N/A	8	N/A	2019
[37]	CV, DPV, CA, Potentiometry	ATxmega32E5	N/A	±100 μA	N/A	2	97 × 66	2018
[38]	CV, LSV, CA	ESP32	±1.5V	±150 μA	N/A	1	N/A	2020
[24]	CV, Amperometry	ATmega32U4	NA	±500 μA	N/A	2	34 × 25	2018

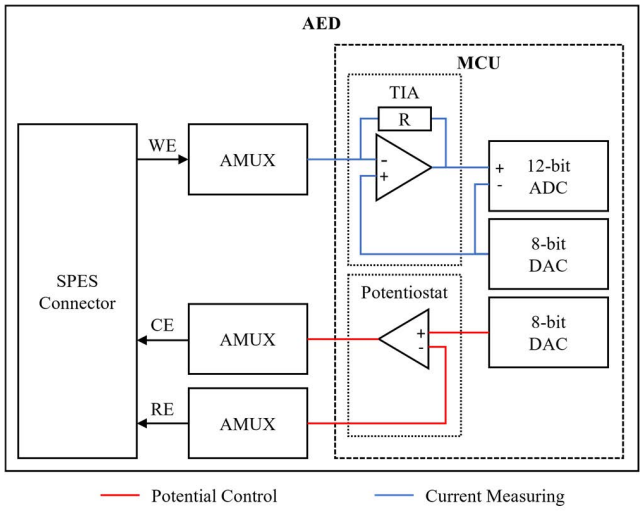

FIGURE 3. Block diagram of the voltammetry, conductometry, and amperometry.

the DAC range, as the common pin. Since the TIA consists of OP-AMP, WE potential should be 2.048 V which is connected to the negative input of the TIA. Therefore, the potential range between WE and RE can be from - 2.048 V to + 2.032 V. With this technique, the AED can provide the potential range from - 2.048 V to + 2.032 V with 16 mV resolution to the sensors. Those can be achieved from OP-AMP's characteristics that the potential difference between two input terminals of OP-AMP is zero, and no current is flowing into the input terminal of the OP-AMP. Among voltammetry, conductometry, and amperometry, the type of analytical methods for the experiment can be decided based on the type of signals from the DAC. For voltammetry and conductometry measurements, a varied potential is provided to sensors, while a constant potential is applied in the case of amperometry.

To process the sensor data in the MCU, I_{sensor} should be converted to voltage and then needs to be digitized, which is the purpose of the current measuring circuit. The WE signal from AMUX is connected to a positive input of TIA that conducts current to voltage conversion. The TIA consists of OP-AMP with a negative feedback resistor ($R_{feedback}$) of 20 KΩ. The converted voltage from TIA is interpreted with a differential 12-bit ADC that can digitize the difference between the two varying voltage levels. The utilized ADC can interpret voltage within a range of ± 2.048 V with 1 mV resolution, which indicates that the proposed AED can detect a 50 nA current difference. I_{sensor} can be obtained by calculation as (1), which is ohm's law (V=IR).

$$I_{sensor} = -\frac{V_{ADC}}{R_{feedback}} \tag{1}$$

where V_{ADC} is the input of ADC. The internal TIA with 20 KΩ of $R_{feedback}$ can convert a current range of ± 100 μA to a voltage range of ± 2 V that can be digitized in the internal ADC. After the conversion, the ADC data is stored in a memory of the MCU. Once the user calls the data, the MCU exports the stored data to the user through wired or wireless communication.

2) POTENTIOMETRY

Potentiometry is an electrochemical technique that measures potential between the two electrodes of electrochemical sensor under a static condition. By tying RE and CE, a two electrodes measurement can be performed. Fig. 4 illustrates the potentiometry block diagram in the AED. The output of the 8-bit DAC is fed into negative input of the ADC and CE/RE as a common pin to make a virtual ground where its output is 2.048 V. The AMUX is implemented to accommodate eight sensors. For measuring the potential of the sensor, which is a voltage gap between WE and RE/CE, differential 12-bit delta-sigma ADC is utilized. The WE potential is connected to a positive input of ADC, while 8-bit DAC is connected to a negative input of ADC to digitize the potential between WE and CE/RE. Once the conversion is done, the data is stored until the user calls it.

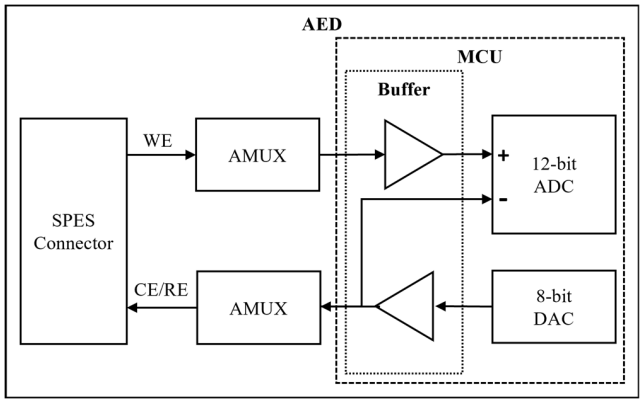

FIGURE 4. Block diagram of the potentiometry.

3) ELECTROCHEMICAL IMPEDANCE SPECTROSCOPY

The EIS requires AC generating block and a current measuring block, and its block diagram is shown in Fig. 5. For the AC generating block, an internal waveform generator supported in the MCU is utilized to generate an arbitrary AC voltage waveform with 32 points per wave. The waveform generator is configured to generate AC voltage which has frequency range of 512 Hz −80 KHz with a 512 Hz resolution, and its peak-to-peak amplitude can be set between 0.5 V and 4 V with a resolution of 0.5 V. To perform the EIS measurement, the applied waveform to a sensor and a converted voltage output of I_{sensor} data are required. Thus, the waveform generator output is connected to both potentiostat's positive input and the negative input of the ADC for measuring the applied waveform while providing the waveform to the RE. The sensor output current is connected to the internal TIA, and its output is fed into ADC to convert the I_{sensor} into the voltage. For wide impedance measurement, the $R_{feedback}$ can be altered from 20 KΩ to 1 MΩ based on the current range. The value of the $R_{feedback}$ can be chosen using customized GUI, which will be described in a later section. Measuring the input and output simultaneously is a key point to measure the phase difference accurately. For this measurement, additional internal direct memory access, counter, and sync blocks are implemented to re-synchronize input signal to the rising edge of the clock signal. To get an efficient and fast conversion, Fast Fourier Transform is embodied in the firmware to obtain real input voltage ($V_{in,Re}{}^2$), imaginary input voltage ($V^2_{in,Im}$), real output voltage ($V^2_{out,Re}$), and imaginary output voltage ($V^2_{out,Im}$) to get the impedance (Z) and phase (θ) information based on (2) and (3). Moreover, to improve accuracy and wide frequency range, the ADC oversampling rate adjustment function is included in the firmware to automatically alter the oversampling rate based on the frequency.

$$|Z| = -\frac{R_{feeback}\sqrt{V^2_{in,Re} + V^2_{in,Im}}}{\sqrt{V^2_{out,Re} + V^2_{out,Im}}} \tag{2}$$

$$\theta = arctan\frac{V_{out,Im}}{V_{out,Re}} - arctan\frac{V_{in,Im}}{V_{in,Re}} - 180° \tag{3}$$

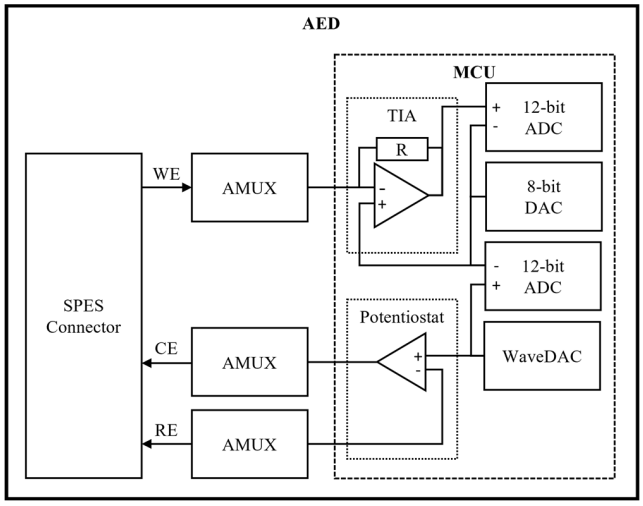

FIGURE 5. Block diagram of the EIS.

C. USER INTERFACE

The proposed AED has the capability to communicate with the user through wired or wireless communication. For wired communication, a customized GUI has been developed. The GUI is written primarily in Python and runs on Windows. It is the primary method to run experiments in the AED, which can control necessary experimental parameters like the value of potential, sweep rate, experiment duration, sensor selection among eight sensors, and number of electrodes selection depending on the type of the experiments. The developed GUI can collect, plot, and store data in Comma Separated Value file format. Additional libraries in Python have been included such as 'Tkinter' for GUI toolkit interface, 'matplotlib' to plot the graph in GUI, 'pyserial' to make a serial communication, 'numpy' for calculation, and 'time' for measuring time to implement mentioned functionalities. An external BLE module is integrated in the device to establish wireless communication. Using the smartphone app which can connect with the BLE device, the user can select the type of the experiments and receive the experimental data.

III. EVALUATION

Fig. 6 illustrates the fabricated and assembled proposed device. The AED is fabricated on a printed circuit board (PCB) and its size is 48 mm × 37 mm. Fig. 6 shows the AED that is a fully populated PCB in a case. The evaluation is done in two phases: electrical testing and chemical testing.

A. ELECTRICAL EVALUATION

Electrical testing has been conducted to evaluate the proposed AED. The electrical evaluation is conducted with a dummy cell consisting of eight resistors as an electrical equivalent model of the sensors, by connecting it with the SPES connectors on the AED board. The AED is connected to the PC using a USB cable, and the customized GUI is utilized to select the experiment type and plot the result with graph as depicted in Fig. 7.

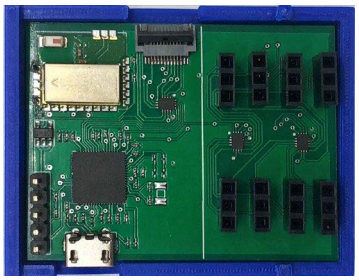

FIGURE 6. Photo of the proposed AED.

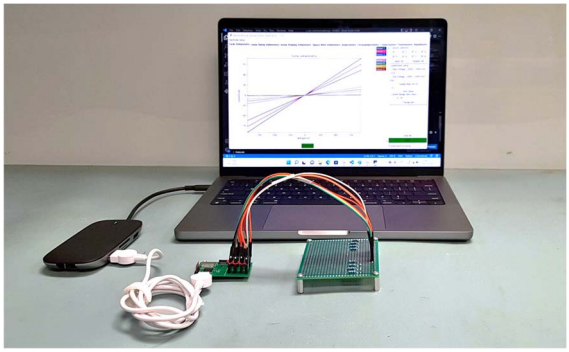

FIGURE 7. Photo of test setup for electrical testing.

1) VOLTAMMETRY

To evaluate the embedded voltammetry methods (CV, LSV, ASV, and SWV), electrical test has been done with dummy cell resistors values are chosen as 10 KΩ, 12 KΩ, 15 KΩ, 22 KΩ, 47 KΩ, 68 KΩ, 100 KΩ, and 1 MΩ. The result of CV, LSV, ASV, and SWV experiments are plotted in the GUI and depicted in Fig. 8, respectively to electrically verify the embedded voltammetry techniques. The Y-axis in the graph of Fig. 8 is current in the unit of μA, while the X-axis is voltage in the unit of mV. For the CV and LSV experiment, the potential sweep range was set from - 900 mV to + 900 mV with a 100 mV/s sweep rate. Since discrete resistors have been utilized to substitute the sensors, the results of the CV and LSV shows the same result which is linear output current with its gradient as provided potential over resistor value as described in Fig. 8(a), (b). In the case of the ASV, the user can set the cleaning voltage, cleaning time, plating time, peak voltage, and sweep rate. The ASV result was obtained when the cleaning voltage was 800 mV, the cleaning time of 60 s, the plating voltage was - 1.5 V, the peak voltage was 500 mV, and the sweep rate was 500 mV/s. Therefore, the linear lines are obtained from ASV experiment as expected from −1.5 V to 500 mV as shown in Fig. 8(c). For the SWV measurement, the potential was swept between – 900 mV to + 900 mV with a 100 mV pulse, step size of 100 mV, and 10 s phase size. The output currents of the measurement are showing pulse property as provided potential is pulse. All the mentioned experimental parameters were set by the right side of the GUI menu. This demonstrated measurement indicates that the designed AED of voltammetry techniques are working as expected based on ohm's law.

2) AMPEROMETRY

The amperometry and CA are implemented as amperometry types of electroanalytical methods in the proposed AED. The same dummy cell used in the voltammetry experiments is utilized for validating the amperometry methods. Fig. 9(a) shows the results of amperometry, while Fig. 9(b) demonstrates results of CA. For the amperometry measurement, a potential of 500 mV was provided to the dummy cell and I_{sensor} was measured by the AED. The X-axis of the graph in Fig. 9 is time in unit of s, and the Y-axis represents the I_{sensor} in unit of μA. The user can set the experiment time in the right section of the GUI, and it was set to 1 minute for the measurement. The expected amperometry results are 50 μA, 41.6 μA, 33.3 μA, 22.7 μA, 10.6 μA, 7.4 μA, 5 μA, and 0.5 μA respectively from (1). In the case of the CA experiment, the start voltage was set to - 900 mV and the end voltage as + 900 mV. Thus, the expected results are ± 90 μA, ± 75 μA, ± 60 μA, ± 41 μA, ± 19.1 μA, ± 13.2 μA, ± 9 μA, and ± 0.9 μA, respectively. Both amperometry and CV results demonstrated in Fig. 9 indicate that the AED can perform the amperometry techniques accurately which match with the expected results.

3) CONDUCTOMETRY

The conductometry testing was done with a dummy resistor array consists of 20 KΩ, 22 KΩ, 27 KΩ, 30 KΩ, 39 KΩ, 47 KΩ, 100 KΩ, and 1 MΩ, whose conductance are 0.05 mS, 0.045 mS, 0.037 mS, 0.03 mS, 0.026 mS, 0.021 mS, 0.01 mS, and 0.001 mS, respectively. The graph's Y-axis is conductance in siemens (S), X-axis is an applied potential to the sensor. The applied potential was selected from 1 V to 2 V with a sweep rate of 100 mV/s in the AED. The selecting display option can be found in the right side of the GUI which gives the user to choose the type of output as either conductance or current. In Fig. 10, the conductometry method in the AED is demonstrated successfully by showing well-matched values with the expected values.

4) POTENTIOMETRY

The Potentiometry validation is conducted with a resistor array as shown in the Fig. 11(a) where the WE1 – WE8 are connected to the WE pin in the AED, the RE/CE of AED are connected to the ground and top of the resistor array. All resistors' values are chosen as 10 KΩ. For the experiment, + 400 mV and – 400 mV were given to the circuit as potential using a power supply unit as shown in Fig. 11(a). Fig. 11(b) illustrates the output results of the potentiometry. User can set experiment time in the GUI, and in this experiment, the time was set to 1 minute. The results are obtained as expected which are - 400 mV, - 300 mV, - 200 mV, - 100 mV, + 100 mV, + 200 mV, + 300 mV, and + 400 mV since Fig. 11(a) is working as voltage divider circuit. Thus, it was proved that the AED could successfully conduct potentiometry.

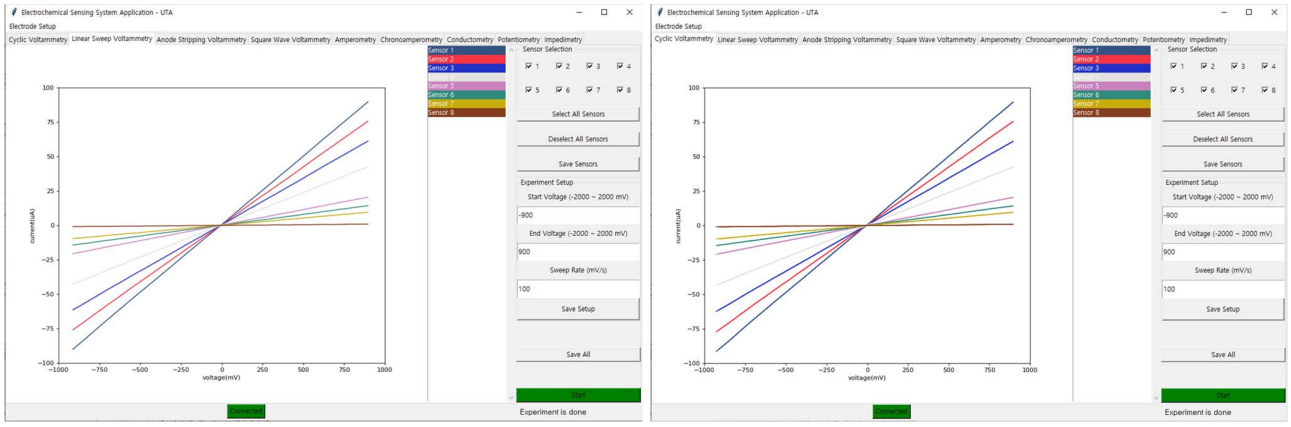

(a) Result of CV

(b) Result of LSV

(c) Result of ASV

(d) Result of SWV

FIGURE 8. Voltammetry results in the customized GUI when the dummy cell is connected to the boards as an electrical equivalent model of the sensors.

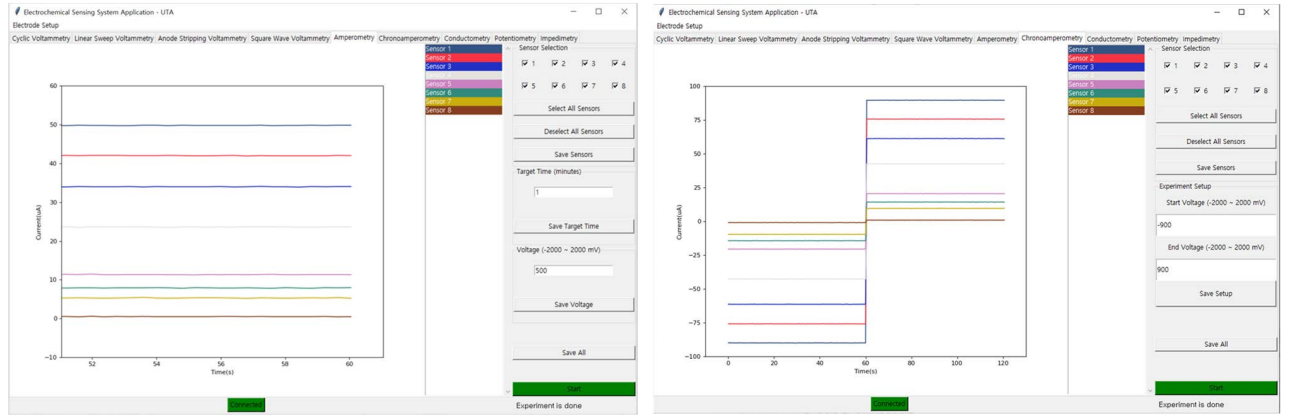

(a) Result of Amperometry

(b) Result of CA

FIGURE 9. Amperometry results in the customized GUI when the dummy cell is connected to the boards as an electrical equivalent model of the sensors.

5) EIS

Unlike other methodologies, the EIS experiment requires AC signal generation in the AED. Therefore, in the custom GUI, the user can select AC voltage where peak-to-peak amplitude range is within 4 V and value of TIA's $R_{feedback}$ can be varied between 20 KΩ and 1 MΩ to conduct accurate measurement for wide range. Also, the GUI can choose the displayed data as impedance or phase. As user friendly GUI, an axis setup

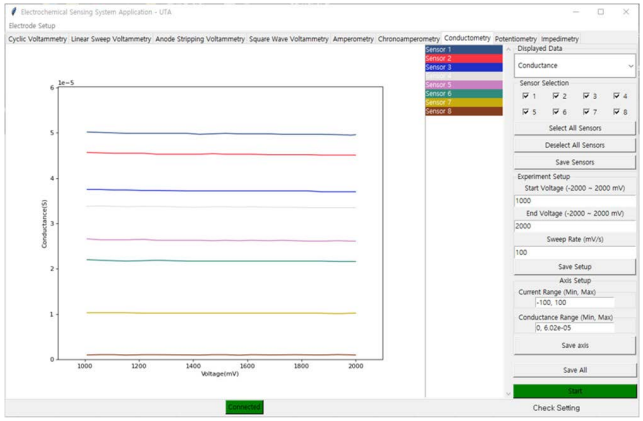

FIGURE 10. Conductometry results in the customized GUI when the dummy cell is connected to the boards as an electrical equivalent model of the sensors.

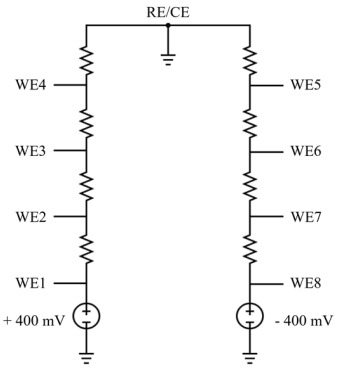

(a) Resistor array circuit used to test potentiometry

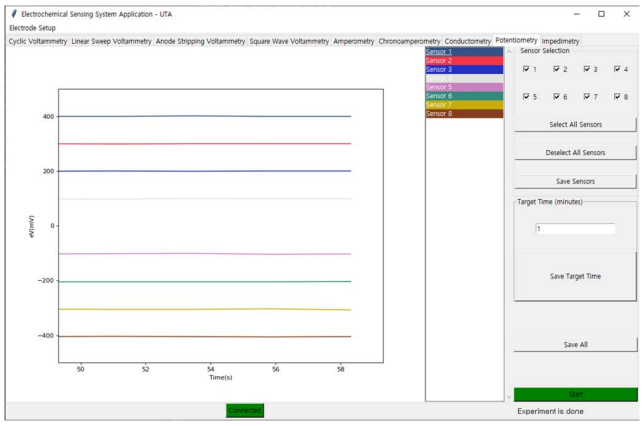

(b) Result of Potentiometry

FIGURE 11. Potentiometry results in the customized GUI when the dummy cell is connected to the boards as an electrical equivalent model of the sensors.

option is included, such as selecting a scale either logarithmic or linear and range of impedance, phase, and frequency. To test the functionality of the EIS, a Randles circuit has been utilized. The Randles circuit, depicted in Fig. 12, is a common equivalent circuit that consists of an R2 in series with the parallel combination of C and R1. For the testing, 20 KΩ is

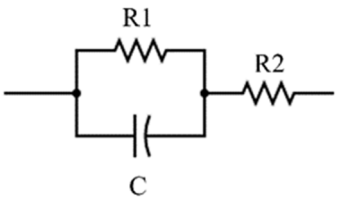

FIGURE 12. Randles circuit.

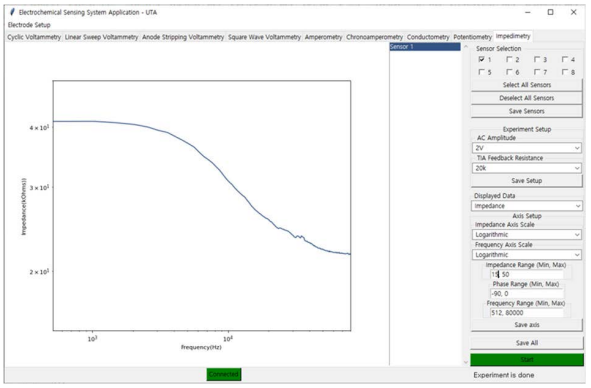

(a) Impedance Plot

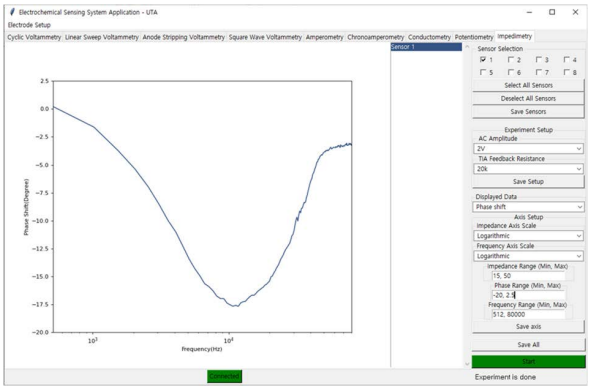

(a) Phase Plot

FIGURE 13. EIS results in the customized GUI when the dummy cell is connected to the boards as an electrical equivalent model of the sensors.

selected as R1 and R2 value while C is 1 nF. Fig. 13 demonstrate the EIS outputs when the Randles circuit is connected instead of the sensor when peak-to-peak amplitude of 2 V is applied, and 20 KΩ is selected as $R_{feedback}$. The graph's X-axis in Fig. 13(a) and (b) is frequency, while the Y-axis is impedance and phase, respectively.

B. CHEMICAL EVALUATION

The experiments were conducted with the electrochemical sensor in order to demonstrate the performance of the AED in real applications. As an example, glucose testing and Uric Acid testing with commercially available sensor were conducted. As commercial SPESs, "DRP-C11L" and

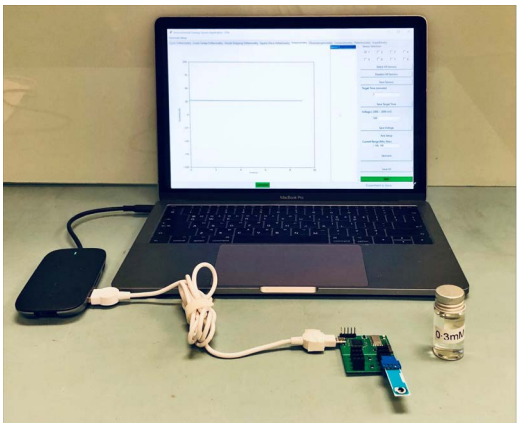

FIGURE 14. Photo of test setup for chemical testing.

"DRP-110CNT" released by Metrohm DropSens (Oviedo, Spain) have been selected for detecting glucose and Uric Acid. The chosen SPESs have three electrodes (WE, CE, and RE). The amperometry method in the AED has been utilized for detecting glucose, while CV technique is implied for detecting of Uric Acid. The test setup of chemical testing is illustrated in Fig. 14. The SPES is inserted into the SPES connector of the AED, and for control and transfer of data, the AED is connected to the PC using a USB cable. The customized GUI is used to perform the experiment and display the sensor data.

1) GLUCOSE TESTING

As a chemical test, the glucose concentration level testing was conducted. An amperometry test was performed with "DRP-C11L" which is general purpose carbon electrodes. The WE and CE of "DRP-C11L" are made of carbon, while RE is available in silver/silver chloride (Ag/AgCl). Glucose solutions of five different concentration (12 mM, 8 mM, 6 mM, 3 mM, and 1.5 mM) are prepared in 0.1 M Tris-HNO3 buffer solution with pH 7.0 to test the amperometry with "DRP-C11L" SPES. In order to the adjust the pH of Tris-HNO3 buffer, nitric acid of 0.1 M concentration was utilized. A 40 μL of each concentration solution was deposited on "DRP-C11L". A fixed potential of + 1 V was applied across RE and CE, and the value of faradic currents across WE are recorded during experiments. Fig. 15(a) illustrates the amperometry test results for 12 mM (Sensor 1), 8 mM (Sensor 2), 6 mM (Sensor 3), 3 mM (Sensor 4), and 1.5 mM (Sensor 5) concentrations of glucose with the proposed AED. The I_{sensor} versus glucose concentration graph is shown in Fig. 15(b), and it shows fairly linear current responses according to varied glucose concentrations.

2) URIC ACID TESTING

The "DRP-110CNT", disposable SPES modified with Carboxyl functionalized Multi-Walled Carbon Nanotubes (MWCNT-COOH), is employed to detect Uric Acid by CV method. The WE of chosen SPES comprises

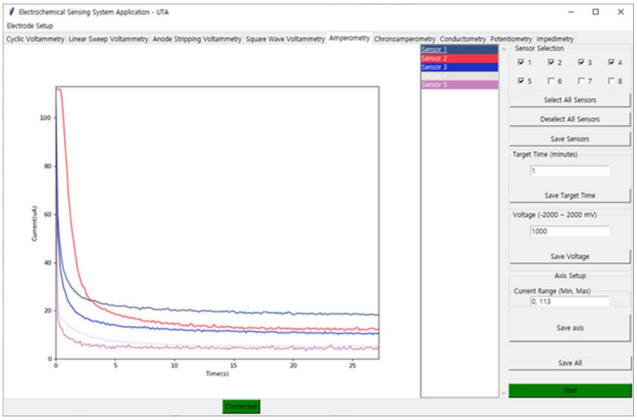

(a) Glucose test result plotted in the customized GUI

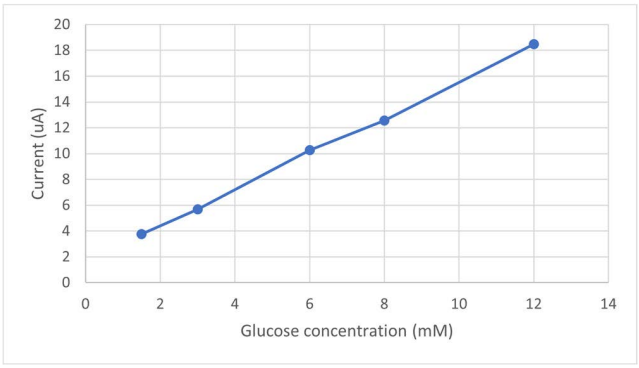

(b) I_{sensor} versus glucose concentration

FIGURE 15. Glucose test result with the proposed device.

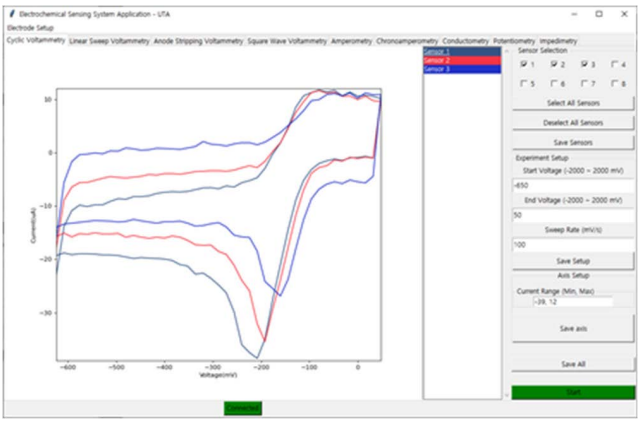

FIGURE 16. Uric acid test result plotted in the customized GUI.

MWCNT-COOH/Carbon, CE with carbon, and RE with silver, respectively. A 50 ml stock solution of 1×10^{-3} M of Uric Acid is prepared by dissolving 8.46 mg of Uric Acid in 0.1 M phosphate buffer of pH 7.0. A sodium hydroxide (NaOH) is used to adjust the pH of the buffer solution. The stock solution is diluted using 0.1 M acetic acid (AcOH/AcO-) of pH 5.0 to obtain lower concentration Uric Acid solutions. As an experimental parameter setup, a sweep voltage from - 600 mV to + 50 mV was selected in the GUI, and it was

applied across RE and CE, with a sweep rate of 100 mV/s. The current values for different concentrations of Uric Acid, which are 1 mM (Sensor 1), 0.7 mM (Sensor 2), and 0.5 mM (Sensor 3) are recorded during the experiment as depicted in Fig. 16. The result demonstrated a higher current flow for higher concentrations and a lower current flow for lower concentrations of Uric Acid, respectively.

IV. CONCLUSION

In this paper, we designed the full-custom AED that can measure eight SPESs simultaneously, performing CV, LSV, ASV, SWV, amperometry, CA, conductometry, potentiometry, and EIS electroanalytical techniques in a single device. The customized, user-friendly GUI is developed to control the device, display electroanalytical methods in real-time, and save the data on the PC. The device can send the data to a smartphone through BLE, and PC using USB communication. Moreover, AED has a very small form factor of 48 mm × 37 mm with sensor connectors that make the AED suitable for portable POC devices. Both electrical and chemical test were conducted to verify the AED performance. The experiment results clearly demonstrate that the designed AED can conduct the above mentioned electroanalytical methods.

REFERENCES

[1] V. Gubala, "Point of care diagnostics: Status and future," *Anal. Chem.*, vol. 84, no. 2, pp. 487–515, Jan. 2012, doi: 10.1021/ac2030199.

[2] Y. Kumar and K. Narsaiah, "Rapid point-of-care testing methods/devices for meat species identification: A review," *Comprehensive Rev. Food Sci. Food Saf.*, vol. 20, no. 1, pp. 900–923, 2021, doi: 10.1111/1541-4337.12674.

[3] A. S. John and C. P. Price, "Existing and emerging technologies for point-of-care testing," *Clin. Biochem. Rev.*, vol. 35, no. 3, pp. 155–167, Aug. 2014.

[4] C. P. Price, "Point of care testing," *BMJ*, vol. 322, no. 7297, pp. 1285–1288, 2001, doi: 10.1136/bmj.322.7297.1285.

[5] M. J. Cima, "Microsystem technologies for medical applications," *Annu. Rev. Chem. Biomolecular Eng.*, vol. 2, no. 1, pp. 355–378, Jul. 2011, doi: 10.1146/annurev-chembioeng-061010-114120.

[6] Marketresearch.com. (Feb. 2021). *Point of Care/Rapid Diagnostics Market by Product (Glucose, Infectious Disease (Hepatitis C, Influenza), Coagulation), Platform (Microfluidics, Immunoassay), Mode of Purchase (Prescription, OTC), Enduser (Hospital, e-Comm, Home Care)—Global Forecast to 2025*. Accessed: Jun. 27, 2022. [Online]. Available: https://www.marketresearch.com/MarketsandMarkets-v3719/Point-Care-Rapid-Diagnostics-Product-14202634/

[7] W. Zhang, R. Wang, F. Luo, P. Wang, and Z. Lin, "Miniaturized electrochemical sensors and their point-of-care applications," *Chin. Chem. Lett.*, vol. 31, no. 3, pp. 589–600, Mar. 2020.

[8] U. Guth, W. Vonau, and J. Zosel, "Recent developments in electrochemical sensor application and technology—A review," *Meas. Sci. Technol.*, vol. 20, no. 4, p. 042002, Jan. 2009.

[9] T. Islam, M. M. Hasan, A. Awal, M. Nurunnabi, and A. J. S. Ahammad, "Metal nanoparticles for electrochemical sensing: Progress and challenges in the clinical transition of point-of-care testing," *Molecules*, vol. 25, no. 24, p. 5787, Dec. 2020.

[10] A. García-Miranda Ferrari, P. Carrington, S. J. Rowley-Neale, and C. E. Banks, "Recent advances in portable heavy metal electrochemical sensing platforms," *Environ. Sci., Water Res. Technol.*, vol. 6, no. 10, pp. 2676–2690, Oct. 2020, doi: 10.1039/D0EW00407C.

[11] F. Cui, Z. Zhou, and H. S. Zhou, "Measurement and analysis of cancer biomarkers based on electrochemical biosensors," *J. Electrochem. Soc.*, vol. 167, no. 3, Jan. 2020, Art. no. 037525, doi: 10.1149/2.0252003jes.

[12] F. R. Beyette, G. J. Kost, C. A. Gaydos, and B. H. Weigl, "Point-of-care technologies for health care," *IEEE Trans. Biomed. Eng.*, vol. 58, no. 3, pp. 732–735, Mar. 2011, doi: 10.1109/TBME.2011.2109251.

[13] L. Zhao, F. Zhao, and B. Zeng, "Synthesis of water-compatible surface-imprinted polymer via click chemistry and RAFT precipitation polymerization for highly selective and sensitive electrochemical assay of fenitrothion," *Biosensors Bioelectron.*, vol. 62, pp. 19–24, Dec. 2014, doi: 10.1016/j.bios.2014.06.022.

[14] A. Hayat and J. L. Marty, "Disposable screen printed electrochemical sensors: Tools for environmental monitoring," *Sensors*, vol. 14, no. 6, pp. 10432–10453, 2014.

[15] A. García-Miranda Ferrari, S. J. Rowley-Neale, and C. E. Banks, "Screen-printed electrodes: Transitioning the laboratory in-to–The field," *Talanta Open*, vol. 3, Aug. 2021, Art. no. 100032, doi: 10.1016/j.talo.2021.100032.

[16] R. Torre, E. Costa-Rama, H. P. A. Nouws, and C. Delerue-Matos, "Screen-printed electrode-based sensors for food spoilage control: Bacteria and biogenic amines detection," *Biosensors*, vol. 10, no. 10, p. 139, Sep. 2020.

[17] A. H. Kamel, A. E.-G.-E. Amr, H. R. Galal, M. A. Al-Omar, and A. A. Almehizia, "Screen-printed sensor based on potentiometric transduction for free bilirubin detection as a biomarker for hyperbilirubinemia diagnosis," *Chemosensors*, vol. 8, no. 3, p. 86, Sep. 2020.

[18] P. S. Pakchin, S. A. Nakhjavani, R. Saber, H. Ghanbari, and Y. Omidi, "Recent advances in simultaneous electrochemical multi-analyte sensing platforms," *TrAC Trends Anal. Chem.*, vol. 92, pp. 32–41, Jul. 2017, doi: 10.1016/j.trac.2017.04.010.

[19] E. Costa-Rama and M. T. Fernández-Abedul, "Paper-based screen-printed electrodes: A new generation of low-cost electroanalytical platforms," *Biosensors*, vol. 11, no. 2, p. 51, Feb. 2021.

[20] P. Yáñez-Sedeño, S. Campuzano, and J. M. Pingarrón, "Integrated affinity biosensing platforms on screen-printed electrodes electrografted with diazonium salts," *Sensors*, vol. 18, no. 2, p. 675, Feb. 2018.

[21] S. I. R. Malha, J. Mandli, A. Ourari, and A. Amine, "Carbon black-modified electrodes as sensitive tools for the electrochemical detection of nitrite and nitrate," *Electroanalysis*, vol. 25, pp. 2289–2297, Sep. 2013, doi: 10.1002/elan.201300257.

[22] B. Attoye, C. Pou, E. Blair, C. Rinaldi, F. Thomson, M. J. Baker, and D. K. Corrigan, "Developing a low-cost, simple-to-use electrochemical sensor for the detection of circulating tumour DNA in human fluids," *Biosensors*, vol. 10, no. 11, p. 156, Oct. 2020.

[23] M. D. M. Dryden and A. R. Wheeler, "DStat: A versatile, open-source potentiostat for electroanalysis and integration," *PLoS ONE*, vol. 10, no. 10, Oct. 2015, Art. no. e0140349, doi: 10.1371/journal.pone.0140349.

[24] S. Parsnejad, Y. Gtat, T.-Y. Lin, X. Liu, P. B. Lillehoj, and A. J. Mason, "Self-ranging thumb-sized multichannel electrochemical instrument for global wearable point-of-care sensing," in *Proc. IEEE 61st Int. Midwest Symp. Circuits Syst. (MWSCAS)*, Aug. 2018, pp. 57–60, doi: 10.1109/MWSCAS.2018.8623887.

[25] A. Ainla, M. P. S. Mousavi, and M. N. Tsaloglou, "Open-source potentiostat for wireless electrochemical detection with smartphones," *Anal. Chem.*, vol. 90, no. 10, pp. 6240–6246, Apr. 2018, doi: 10.1021/acs.analchem.8b00850.

[26] A. F. D. Cruz, N. Norena, A. Kaushik, and S. Bhansali, "A low-cost miniaturized potentiostat for point-of-care diagnosis," *Biosensors Bioelectron.*, vol. 62, pp. 249–254, Dec. 2014, doi: 10.1016/j.bios.2014.06.053.

[27] M. W. Glasscott, M. D. Verber, J. R. Hall, and A. D. Pendergast, "SweepStat: A build-it-yourself, two-electrode potentiostat for macroelectrode and ultramicroelectrode studies," *J. Chem. Educ.*, vol. 97, no. 1, pp. 265–270, 2020, doi: 10.1021/acs.jchemed.9b00893.

[28] J. Jung, J. Lee, S. Shin, and Y. Kim, "Development of a telemetric, miniaturized electrochemical amperometric analyzer," *Sensors*, vol. 17, no. 10, p. 2416, Oct. 2017.

[29] Y. Montes-Cebrián, A. Álvarez-Carulla, G. Ruiz-Vega, J. Colomer-Farrarons, M. Puig-Vidal, E. Baldrich, and P. L. Miribel-Català, "Competitive USB-powered hand-held potentiostat for POC applications: An HRP detection case," *Sensors*, vol. 19, no. 24, p. 5388, Dec. 2019.

[30] D. M. Jenkins, B. E. Lee, S. Jun, J. Reyes-De-Corcuera, and E. S. McLamore, "ABE-stat, a fully open-source and versatile wireless potentiostat project including electrochemical impedance spectroscopy," *J. Electrochem. Soc.*, vol. 166, no. 9, pp. B3056–B3065, 2019, doi: 10.1149/2.0061909jes.

[31] P. Lopin and K. V. Lopin, "PSoC-stat: A single chip open source potentiostat based on a programmable system on a chip," *PLoS ONE*, vol. 13, no. 7, Jul. 2018, Art. no. e0201353, doi: 10.1371/journal.pone.0201353.
[32] L. Yang and T. Chen, "A handheld electrochemical sensing platform for point-of-care diagnostic applications," in *Proc. IEEE Biomed. Circuits Syst. Conf. (BioCAS)*, Oct. 2017, pp. 1–4, doi: 10.1109/BIOCAS.2017.8325052.
[33] K. J. Land, D. I. Boeras, X.-S. Chen, A. R. Ramsay, and R. W. Peeling, "REASSURED diagnostics to inform disease control strategies, strengthen health systems and improve patient outcomes," *Nature Microbiology*, vol. 4, no. 1, pp. 46–54, Jan. 2019, doi: 10.1038/s41564-018-0295-3.
[34] C. Dincer, R. Bruch, A. Kling, P. S. Dittrich, and G. A. Urban, "Multiplexed point-of-care testing–xPOCT," *Trends Biotechnol.*, vol. 35, no. 8, pp. 728–742, Aug. 2017, doi: 10.1016/j.tibtech.2017.03.013.
[35] D. Wu, D. Rios-Aguirre, M. Chounlakone, S. Camacho-Leon, and J. Voldman, "Sequentially multiplexed amperometry for electrochemical biosensors," *Biosensors Bioelectron.*, vol. 117, pp. 522–529, Oct. 2018, doi: 10.1016/j.bios.2018.06.049.
[36] S. T. Rajendran, E. Scarano, and M. H. Bergkamp, "Modular, lightweight, wireless potentiostat-on-a-disc for electrochemical detection in centrifugal microfluidics," *Anal. Chem.*, vol. 91, no. 18, pp. 11620–11628, Sep. 2019, doi: 10.1021/acs.analchem.9b02026.
[37] I. N. Hanitra, L. Lobello, F. Stradolini, A. Tuoheti, F. Criscuolo, T. Kilic, D. Demarchi, S. Carrara, and G. De Micheli, "A flexible front-end for wearable electrochemical sensing," in *Proc. IEEE Int. Symp. Med. Meas. Appl. (MeMeA)*, Jun. 2018, pp. 1–6, doi: 10.1109/MeMeA.2018.8438787.
[38] S. Sarkar and M. Bhattacharya, "SStat: Wi-Fi and Bluetooth integrated multimodal 'do-it-yourself' electrochemical potentiostat," in *Proc. 46th Annu. Conf. IEEE Ind. Electron. Soc. (IECON)*, Oct. 2020, pp. 5249–5254, doi: 10.1109/IECON43393.2020.9254701.

HYUSIM PARK received the B.S. and M.S. degrees in electronics engineering from Kyung Hee University, Yongin, South Korea, in 2014 and 2016, respectively, and the Ph.D. degree in electrical engineering from The University of Texas at Arlington, Arlington, TX, USA, in 2021. She is currently a Postdoctoral Researcher with the Department of Electrical Engineering, The University of Texas at Arlington. Her research interests include embedded system design and system on a CMOS IC chip for electrochemical sensing application.

YOUNGHUN PARK received the B.S. and M.S. degrees in mechanical engineering from Kyung Hee University, Yongin, South Korea, in 2017 and 2019, respectively. He is currently pursuing the Ph.D. degree with the Department of Electrical Engineering, The University of Texas at Arlington, Arlington, TX, USA. His research interests include sensing embedded systems, mobile app, graphic–user interface, and machine learning.

SHANTHALA AKSHMINARAYANA (Graduate Student Member, IEEE) received the B.E. degree in electronics engineering and the M.Tech. degree in VLSI and embedded systems from Visvesvaraya Technological University, Karnataka, India, in 2015 and 2017, respectively. She is currently pursuing the Ph.D. degree with the Department of Electrical Engineering, The University of Texas at Arlington, Arlington, TX, USA. She worked as a Digital Design Engineer at Intel Technologies India Pvt. Ltd., Karnataka, from 2017 to 2018. Her research interests include sensing embedded systems and CMOS sensing system on a chip.

HYUN-MIN JUNG received the Ph.D. degree from the School of Electronics Engineering, Kyungpook National University, South Korea, in 2020. He is currently a Senior Researcher with the Electrochemistry Department, Korea Institute of Materials Science (KIMS), South Korea. His current research interests include the study of sensors based on semiconductor devices and its applications to taste sensors, gas sensors, biosensors, and pH-ion sensors.

MIN-YEONG KIM received the Ph.D. degree in electrochemistry from Pusan National University, Republic of Korea, in 2019. She is currently a Postdoctoral Researcher with the Department of Electrochemistry, Korea Institute of Materials Science (KIMS). Her research interests include the synthesis of electrochemical nano-catalysts and the various advanced applications and nanotechnology, including electrochemical sensors, biosensor, and surface analysis.

KYU HWAN LEE received the B.S. and M.S. degrees in materials engineering from Hanyang University, and the Ph.D. degree in materials science and engineering from the Korea Advanced Institute of Science and Technology (KAIST). He is currently a Professor of advanced materials engineering at the University of Science and Technology and a Principal Researcher with the Department of Electrochemistry, Korea Institute of Materials Science (KIMS). His research interests include the synthesis of electrochemical nanomaterials and the implementation of these materials in various advanced applications, including electrodeposition, sensors, catalysts, electrode, and water treatment application.

SUNGYONG JUNG (Senior Member, IEEE) received the B.S. and M.S. degrees in electronics engineering from Yeungnam University, Kyeongsan, South Korea, in 1991 and 1993, respectively, and the Ph.D. degree in electrical engineering from the Georgia Institute of Technology, Atlanta, GA, USA, in 2002.

He was an Advanced Circuit Engineer at Quellan Inc., Atlanta, from 2001 to 2002. He is currently an Associate Professor with the Department of Electrical Engineering, The University of Texas at Arlington. His research interests include IC and system design for chemical/bio-applications, system design for precision agriculture, RF IC and system design for wireless communications and radar applications, high-speed CMOS analog and mixed-signal circuit design, and optoelectronic IC design.